NANOHYDROXYAPATITE PREPARED BY RAPID PRECIPITATION METHOD IN THE PRESENCE OF TETRABUTYLAMMONIUM HYDROXIDE

Ľ. Medvecký, J. Briančin, J. Ďurišin

Abstract

Nanohydroxyapatite with a Ca/P ratio close to 1.66 was prepared by the rapid precipitation of ethanol calcium ion and orthophosphoric acid solutions in the presence of tetrabutylammonium hydroxide (TBAOH). The TBAOH acted as strong base for the fine calcium hydroxide suspension formation and auxiliary agent for carbonated hydroxyapatite formation. A very fine amorphous calcium phosphate phase with a large specific surface (around 110 m^2/g) was prepared. The more than 80% of nanohydroxyapatite agglomerates were under 0.8 μm in size. The apatite-like phase precipitation was significantly influenced by the TBAOH adsorption on apatite particle surfaces. The stability of hydroxyapatite in water and during thermal treatment was studied, where the strong apatite lattice disordering was verified in annealed samples at 600°C and the pure hydroxyapatite was created after annealing at 950°C.

Keywords: biomaterials, hydroxyapatite, amorphous calcium phosphate, precipitation, infrared spectroscopy (IR)

INTRODUCTION

The hydroxyapatite ($Ca_5(PO_4)_3OH$) is the main inorganic compound of hard tissues in the body. Bone crystallites are extremely small and contain impurities, such as carbonate (4–6% carbonate), sodium and magnesium ions as the result of their incorporation into the structure [1]. Some effects such as the purity of raw material [2], atmosphere, pH [3], temperature, aging time [4,5] on morphology and crystallinity of hydroxyapatite nanoparticles were evaluated. The carbonated hydroxyapatite (CHA) is more appropriate material for bone defect filling or as coating on metal substrates than the stoichiometric hydroxyapatite because of higher bioactivity, earlier bioresorption and similarity to apatite in bone [6]. The high CO_3^{2-} content in CHA was achieved (up to 12 mass.%) by the precipitation of CHA drop by drop of reagent water solutions to ammonium solution (pH~12) and stirring at elevated temperature in the reactor [7]. Rajabi-Zamani et al. [8] examined to prepare hydroxyapatite from non-alkoxide precursors in ethanol, where the carbonated hydroxyapatite with a small amount of the β-tricalcium phosphate was obtained after annealing at 750°C. Tung et al. [9] showed that the amorphous calcium phosphate (ACP) is formed in ethanol-water solutions and the Ca/P ratio of ACP increased with the pH from 1.28 (at pH 7.4) to 1.50 (at pH 10.2). In aqueous solutions, the ACP rapidly transforms to poorly crystallized hydroxyapatite at pH 7.4. Ikawa et al. [10] observed the formation of lamellar mesostructured calcium phosphates using n-alkylamines ($n\text{-}C_nH_{2n+1}NH_2$, n = 8–18) at room temperature in the mixed solvent systems of aliphatic

Ľubomír Medvecký, Juraj Ďurišin, Institute of Materials Research, Slovak Academy of Sciences, Košice, Slovak Republic
Jaroslav Briančin, Institute of Geotechnics, Slovak Academy of Sciences, Košice, Slovak Republic

alcohol (C_nH_{2n}+1OH, n = 1–4) and water. Crooks et al. [11] found the hydrogen carbonate ions are formed with the reaction of tertiary amines and CO_2 in water solutions.

In this paper, the formation of ACP, the transformation and stability of nanohydroxyapatite (HAP) prepared from calcium and phosphate precursors in alcohol solutions with an addition of tetrabutylammonium hydroxide as a strong base were studied. This preparation method has not yet been studied in papers and some specific features of the prepared HAP are shown in the manuscript.

EXPERIMENTAL MATERIALS AND METHODS

Preparation of HAP

The HAP was synthesized by the precipitation of calcium suspension and orthophosphoric acid (85%, analytical grade, Sigma–Aldrich, USA) dissolved in ethanol (0.5 $mol \cdot dm^{-3}$ solutions) with Ca/P ratio equals 1.667. The calcium suspension was obtained by mixing of tetrabutylammonium hydroxide (TBAOH, for synthesis, 12.5% methanol solution, Merck KGaA, Darmstadt, Germany) with $CaCl_2.2H_2O$ ethanol (absolute, analytical grade, Sigma–Aldrich, USA) solution (0.5 $mol \cdot dm^{-3}$) in an amount corresponding to full substitution of chloride ions for OH^- during the interaction of reagents. The HAP precipitation was carried out by a slow addition of the orthophosphoric acid solution to calcium suspension at 25°C in a magnetic stirrer for 2 hours. The rotation speed of the stirrer was kept at 300 rpm. After mixing, the precipitate was filtered over the membrane filter (PVDF, Millipore, USA, pore size < 0.22 μm), washed with ethanol and dried at 80°C for 48 hours. The part of prepared HAP was immersed into distilled water for 15 minutes at 25°C (for the analysis of the effect of water on HAP stability), filtered and dried at 80°C for 3 hours.

The phosphorus concentration in solution was determined by the calorimetry as P-Mo-V complex (UV VIS spectrophotometer, HITACHI 1100 U, Japan). The Ca^{2+} ion content in samples was determined by the complexometric titration (EDTA, Ca^{2+} ion selective electrode (Theta 90, Czech Republic) was used to determine the equivalence point). The CO_3^{2-} content in HAP was determined by volumetric method (the absorption of CO_2 with KOH solution) after the thermal decomposition of HAP at temperatures up to 1300°C [12].

The phase composition of powder samples was analysed using X-ray diffraction analysis (XRD, Philips, X´Pert Pro, CuKα radiation), infrared spectroscopy (SPECORD M80, Carl-Zeiss Jena, Germany, 1 mg sample + 400 mg KBr), thermogravimetric analysis and differential scanning calorimetry (Mettler 2000C). Specific surfaces of hydroxyapatites were measured by the BET method (N_2 adsorption at −196°C, GEMINI, Micromeritics, USA). The particle size distribution was done by the Nanophox (SYMPATEC HELOS, Sympatec GmbH, Germany) particle size analyzer. The morphology and particle size of HAP were observed by transmission electron microscopy (TEM, TESLA 500, Czech Republic). The average particle size was calculated from the size of 300–350 particles observed by TEM.

RESULTS AND DISCUSSION

HAP particles after drying (Fig.1a) had a spherical or needle-like shape with an average size about 20 nm. The particle size and morphology were partially changed after their washing with water (HAPW) for 15 minutes at 25°C and drying at 80°C for 8 hours. The spherical or regular shaped HAPW particles with sizes of 40-70 nm were observed in HAPW sample (in Fig.1b) with only a small fraction of origin particle agglomerates. After

annealing of HAP or HAPW samples at 600°C for 30 min, the particle size increased to 80-125 nm and regular shaped particles were found by TEM (Fig.1c). The changes in the particle size of the HAP and HAPW powder samples after washing in water or annealing correspond with the measured values of their specific surfaces, which decreased from 110 to 84 (HAPW) or to 18 m^2/g (annealed HAP). The calculated average particle sizes from the sample`s specific surfaces (the spherical particle morphology approximation) rose from 17 nm (original HAP) to 25 nm (HAPW) or 105 nm (annealed HAP) which are in good agreement with the TEM observations of particles. The distribution of HAPW particle agglomerates is shown in Fig.2. Four maxima can be seen on the distribution curve whereas agglomerates with a size from 200 to 400 nm and from 400 to 800 nm represent almost 80% of the particle amount (x_{50} = 503 nm). The agglomerate sizes are significantly lower than what had been found by Hammari et al. [13] in the case of hydroxyapatite prepared by the precipitation from calcium hydroxide water-ethanol suspension. Probably reason for such lowering of nanoparticle agglomeration was the TBAOH adsorption on hydroxyapatite particles` surfaces.

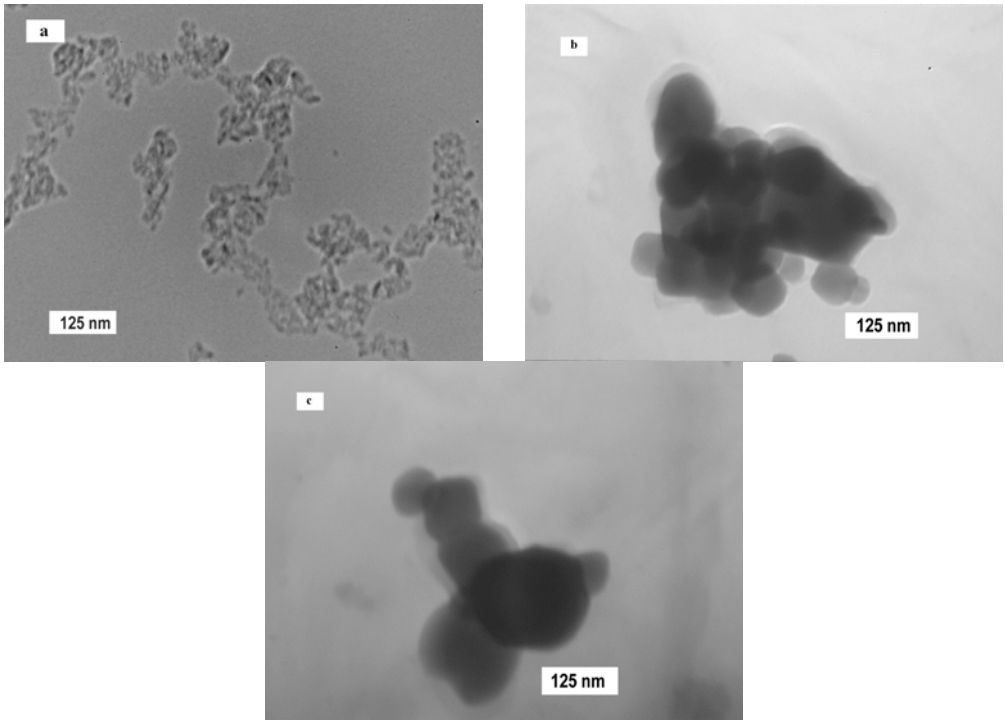

Fig.1. TEM micrographs of HAP as prepared (a), HAPW (b) and consequently annealed at 600°C for 30 minutes.

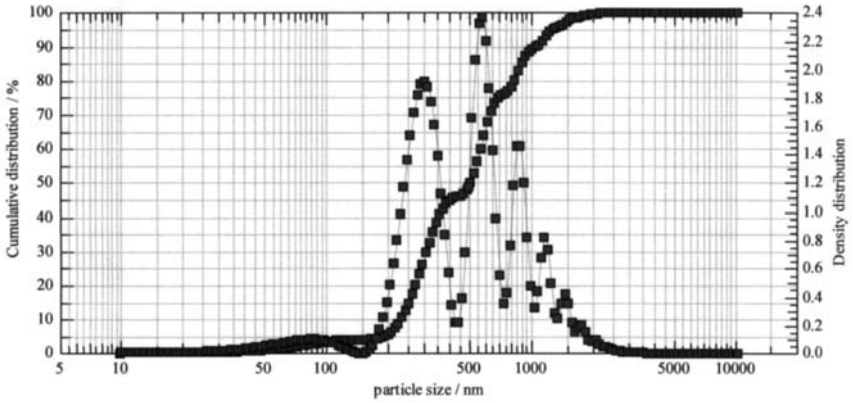

Fig.2. Particle size distribution in HAPW.

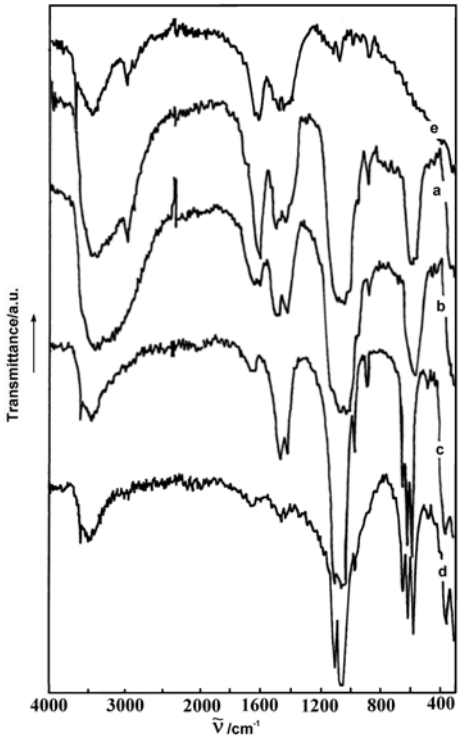

Fig.3. IR spectra of HAP as prepared (a), HAPW (b), HAP annealed at 600°C for 30 minutes (c), HAP annealed at 950°C for 10 minutes (d), precipitated calcium hydroxide (e).

IR spectra of precursors and HAP are shown in Fig.3 and characteristic vibration bands are summarized in Tab.1. The characteristic bands of N-O stretching vibration (1600-1800 cm^{-1}), CH stretching (2880, 2980 cm^{-1}), CH_2- , CH_3-s bending vibrations (1450 and 1500 cm^{-1}) of TBAOH are visible in the HAP spectrum (Fig.3a) [14,15]. These bands have significantly lower intensities in the HAPW spectrum (Fig.3b) which verifies partial TBAOH desorption from the surface of particles. The broad band around 3450 cm^{-1}

indicates adsorbed H_2O whereas the other H_2O band at 1650 cm^{-1} in HAP and HAPW spectra is overlapped with TBAOH (N-O) vibrations. The peak area of H_2O is higher in the HAPW spectrum, which corresponds with the adsorption of water molecules on HAP particle surfaces after soaking in water. Besides that, the characteristic antisymmetric (ν_3) and symmetric (ν_1) P-O stretching vibrations of PO_4^{3-} group (located at 1050, 1100 and 962 cm^{-1}), O-P-O bending (ν_4) vibrations (565 and 603 cm^{-1}) can be found in both spectra [16], but they are not distinctly separated. This fact clearly indicates the formation of amorphous calcium phosphate [17]. ν_2 and ν_3 modes of CO_3^{2-} (870 and 1400-1500 cm^{-1}) are overlapped with TBAOH vibrations, the librational mode (630 cm^{-1}) and stretching vibration (3570 cm^{-1}) of OH hydroxyapatite group [18] are not visible in HAP and HAPW spectra. Vanishing TBAOH bands in the IR spectrum of the origin HAP sample after annealing at 600°C for 30 minutes in air fully manifests the TBAOH adsorption on HAP (Fig.3c). There can be clearly observed a significant decrease in band intensities of physisorbed water (3450 cm^{-1} and 1650 cm^{-1}) but they can be still visible in spectrum. Side peaks which correspond to CO_3^{2-} group vibrations (1420, 1460 and 870 cm^{-1}) can be also resolved. PO_4^{3-} group vibration bands were split into several maxima at 1060, 1100, 960, 570, 600 cm^{-1} and OH hydroxyapatite vibrations (3570 and 630 cm^{-1}) can be distinguished, which confirms the recrystallization and stabilization of the lattice. After annealing a sample at 950°C for 10 min., the traces of CO_3^{2-} group vibration bands are only present in the HAP spectrum (Fig.3d), whereas peaks of all other PO_4^{3-} group vibrations were unchanged. From detailed analysis of carbonate bands it results that the AB type of HAP is formed after annealing at 600°C (intensively peak at 1470 cm^{-1} then at 1420 cm^{-1}, shoulder at 1520-1550 cm^{-1}) [18]. Note that the HAP is precipitated via the calcium hydroxide, which is created by the interaction between Ca^{2+} and OH^- (from TBAOH) ions as it results from the IR spectrum in Fig.3e (peak at 3680 cm^{-1} of stretching OH vibrations of $Ca(OH)_2$) [19]. Besides this, other bands (2800-3000, 1600-1700, 1400-1500, around 1100 and 880 cm^{-1}) from vibrations of adsorbed TBAOH on calcium hydroxide particles can be also found in spectrum. The TG analysis of created calcium hydroxide showed the adsorbed TBOH amount was around 8 mass.%.

Tab.1. Characteristic band of bond vibrations found in IR spectra.

Wave number/cm^{-1}	Assignment
3680	OH stretching in $Ca(OH)_2$
3570	stretching vibrations of OH in HAP
3450	adsorbed H_2O
2880, 2980	CH stretching in TBAOH
1600-1800	stretching vibration of NO group of TBAOH
1650	vibrations from physisorbed H_2O
1520, 1550	AB-type; (ν_3) vibrations mode of CO_3^{2-}
1450 -1500	CH_2- , CH_3-groups, bending
1470-1420	B-typ; (ν_3) vibrations mode of CO_3^{2-}
1050, 1100	P-O (ν_3) asymetric PO_4^{3-} stretching vibration
962	P-O (ν_1) symetric PO_4^{3-} stretching vibration
870	(ν_2) vibrations mode of CO_3^{2-}
630	P-OH deformation vibration in HAP
~603, ~565	O-P-O (ν_4) symetric PO_4^{3-} bending vibration

On the TG curve of HAP (Fig.4a), four regions of mass losses were found - approx. 9 mass.% up to 180°C characteristic for the physisorbed water release (endo-effect on DSC curve), 16 mass.% between 180-400°C represents the decomposition of TBAOH species adsorbed (or bonded) on particle surfaces (small exo-effect on DSC curve), 0.9 mass.% from 540 to 650°C (discussed later) and 9.5 mass.% in the region from 780 to 950°C (endo-effect on DSC curve), which is characteristic for the CO_2 release from the decomposition of carbonates and water from the crystalline structure of HAP. After annealing of HAP at 600°C for 30 min. (Fig.4b), two regions were observed only - 4 mass.% losses were found around 250°C from the desorption of physisorbed water only and 9 mass.% losses were measured by TG analysis up to 950°C, which clearly indicates the decomposition of adsorbed TBAOH but practically no change in carbonate content. The quantitative CO_2 chemical analysis of this sample showed none and 5.57±0.08 mass.% CO_2 evolution at 700°C and 1300°C respectively, which corresponds to 7.6 mass.% CO_3^{2-} and 3.4 mass.% H_2O (calculated from the difference between TG losses and CO_2 content at 950°C).

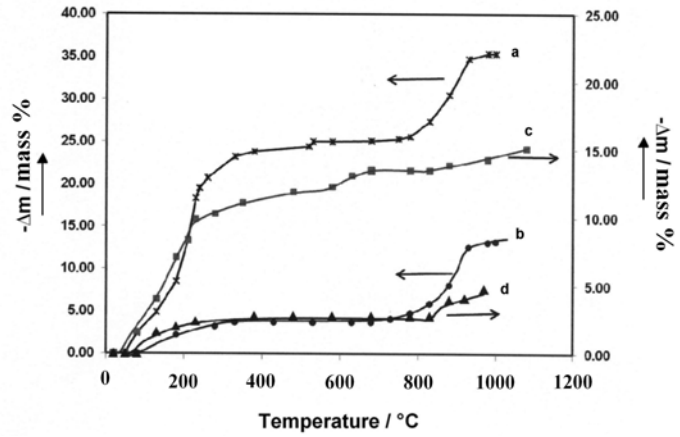

Fig.4. TG analysis of HAP as prepared (a), HAP annealed at 600°C for 30 minutes (b), HAPW (c), HAP annealed at 600°C for 10 minutes and soaked in water for 15 minutes (d).

Significant changes on TG HAP curve were found after washing with water for 15 min (Fig.4c). The first mass loss up to 180°C increased to 12 mass.% but it was partially overlapped with losses caused by the decomposition of TBAOH (around 3 mass.% from 180 to 400°C, confirmed the CO_2 evolution). The lower losses in this region are in accordance with TBAOH content reduction resulting from IR analysis. A very slow rate of carbonate decomposition in HAPW (in comparison with HAP) was observed at the temperature region above 800°C. This is evidence of the low stability of apatite-like phase in HAP and some HAPW lattice rearrangement during soaking the origin sample in water. The mass losses between 540 and 650°C increased up to approx. 1.6 mass.% in comparison with HAP. We believe that these mass losses are caused by the substitution of a certain amount of carbonates for OH^-, which is accompanied with CO_2 release (2 mass.% determined by the volumetric method between 500 and 700°C). A small exoeffect was also observed on the DSC curve, which could verify the lattice transformation and recrystallization of HAPW amorphous nanoparticles. The 3.74 ± 0.10 mass.% and 3.11±0.08 mass.% CO_2 content in sample were found by the volumetric method at 700°C

and 1300°C from which it results that the TBAOH adsorbed amount was around 2.4 mass.% (after subtraction of mass losses between 540-650°C) and the carbonate content in HAPW was 4.25 mass.%. When the HAP sample annealed at 600°C was soaked in water for 15 minutes (Fig.4d), the detected CO_2 amount (volumetric analysis) dropped to 0.8 mass.% at a temperature of 950°C and 3.0±0.1 mass.% at 1300°C (Tab.2, sample HAP 600°C+W), which represents approx. 4.1 mass.% of carbonates in the sample. It is clear from comparison that the TBAOH adsorbed amount significantly fell down by washing HAP nanoparticles in water and similarly, the stability of carbonates in water was very low and independent of the thermal treatment of samples up to 600°C.

Tab.2. Results of TG and volumetric analysis of samples.

Temperature range [°C]	HAP	HAPW		HAP 600°C		HAP 600°C+W	
	TG[a] [mass.%]	TG [mass.%]	VM[b] [mass.%]	TG [mass.%]	VM [mass.%]	TG [mass.%]	VM [mass.%]
< 200	9	12	-	4	-	3	-
180-400	16	3	1.74	-	-	-	-
540-650	0.9	1.6	2	-	-	-	-
780-950	9.5	-	- 3.11 at 1300°C	9	- 5.6 at 1300°C	1.5	0.8 3.0 at 1300°C

[a] mass losses from TG analysis
[b] CO_2 content in sample determined by volumetric analysis

XRD analysis of the HAPW and HAPW annealed at 600°C are shown in Fig.5. As it can be visible in the figure, the wide peaks of HAPW between 2θ = 25-35 and 45-50° correspond to almost fully amorphous apatite-like calcium phosphate phase [9]. Such an amorphous phase (with particle size < 20 nm) with extremely deformed lattice has the highly-active surface and inner structure for recrystallization and lattice rearrangement. After the samples were annealed, typically XRD patterns of hydroxyapatite (ICDD PCD4 01-071-5048) or carbonated hydroxyapatite (ICDD PCD4 01-075-3727) were observed. The crystallinity size of annealed samples calculated from reflections of (002) plane using the Scherrer equation were 30 nm and 40 nm in the HAP and HAPW samples respectively. The lattice parameters from both patterns were determined by the Rietveld method (Rietica, LHPM program [20]. At the first step 2θ zero point, unit cell constants were refined together with the simulation of the background and peak shape using, respectively, 6th-order polynomial and asymmetric pseudo-Voigt functions. The refinement of the structure was carried out in the space group *P*63/*m* and input parameters for calculation and model structure were used according to Ivanova et al. [21], where the split position of the O3 atom made it possible to find two orientations of CO_3 triangles sharing one of their edges. They occupy randomly the adjacent faces of a PO_4 tetrahedron which are parallel to the *c* axis. This model better fitted the experimental XRD patterns of our samples than the face model with CO_3 triangles located equally between the two mirror plane related faces of the vacated phosphate tetrahedron [22].

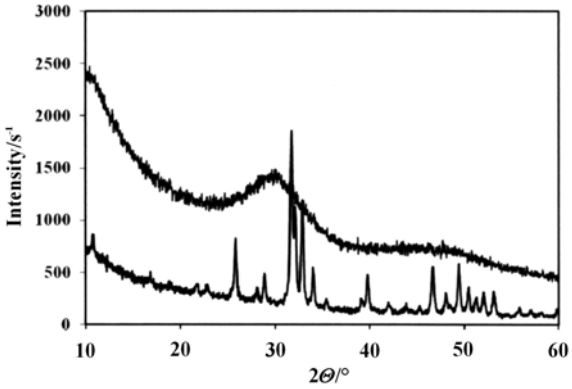

Fig.5. XRD analysis of HAPW (upper curve) and HAPW annealed at 600°C for 30 minutes (lower curve).

The result of Rietveld XRD pattern refinement of HAPW annealed at 600°C for 30 minutes is shown in Fig.6. The lattice parameters (a, c) of HAP and HAPW were 9.4192(2), 6.8898(1) respectively 9.4283(3), 6.8893(2). From the comparison of XRD patterns with standards it results that the parameters of HAPW are very close to pure hydroxyapatite a = 9.425 and c = 6.884 (ICDD PCD4 01-071-5048) whereas the HAP lattice parameter decreased, which may verify the formation of B-type carbonated hydroxyapatite [23]. The strong PO_4 tetrahedra distortion was found in both types of samples with the presence of vacancies in Ca1, O1 and O2 sites and lower P occupancy (0.9084, 0.9452) in HAP than HAPW sample which corresponds with the higher CO_3^{2-} content in the lattice. In both samples, the higher OH occupancies and temperature factors than in stoichiometric hydroxyapatite were determined, which may verify the presence of water molecules in channels [21,23]. From the chemical analysis and IR spectroscopy results the unsurprising fact that small water amounts were really present in the sample`s inner structures after annealing at 600°C. We assumed that applied temperature is not sufficient from the point of view of the complete structural rearrangement in these samples. It has to be taken into consideration that a relatively large amount of TBAOH was adsorbed on the particle surfaces, which inhibited rapid growth and recrystallization of HAP particles during thermal treatment (caused e.g. by the gas evolution). The adsorbed TBAOH significantly affects on the precipitation of hydroxyapatite nanoparticles from alcohol solutions, where the surface hydrophobicity of precipitated particles rises after interaction between polar amino groups in tertiary amine with the basic surface of apatitic calcium phosphate, as a result of the formation of fine amorphous particles observed in TEM micrographs and lowering degree of the particle agglomeration. The strongly disordered HAP lattice was verified by the XRD analysis and unresolved bands of phosphate groups were observed in IR spectra [9]. Apart from the significant instability of prepared HAP in water, it was confirmed by both the rapid decrease of CO_3^{2-} content (about 50%) after its immersion into water and the carbonate decomposition shift to higher temperatures. The carbonates are created - firstly by the effective mutual interaction of CO_2 from air and TBAOH (hydrogencarbonate ions formation) [11], secondly the similar reaction with very fine amorphous $Ca(OH)_2$ particles, and thirdly, the surface $CO_2(g)$ absorption by the created amorphous calcium phosphate during the thermal decomposition of adsorbed TBOH molecules at lower temperatures. Note that carbonated nanohydroxyapatite with the given Ca/P ratio was prepared by precipitation during 2 hours and no further ageing was used.

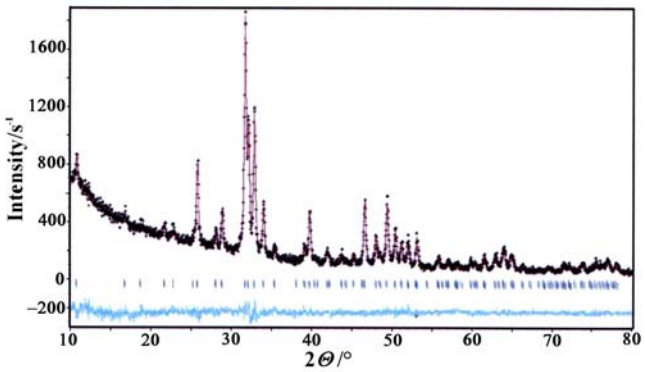

Fig.6. XRD pattern Rietveld refinement of HAPW annealed at 600°C for 30 minutes**.**

The Ca/P ratio determined by the chemical analysis of HAPW was 1.66±0.02 was very close to ratio in pure hydroxyapatite. The final HAPW formula after annealing at 600°C calculated on a chemical analysis basis (the contents of Ca, P, CO_3^{2-} and water in sample were 37.1±0.2, 17.2±0.2, 4.11±0.05 and 4.0±0.1 mass.% respectively) and the charge balance can be given as $Ca_{4.42}(PO_4)_{2.66}(CO_3)_{0.34}(OH)_{0.18}$, where the remaining water content was not included into the calculation. The unit cell content of the sample $Ca_{4.64}(PO_4)_{2.83}(CO_3)_{0.17}$ $[(OH)_{0.13}(CO_3)_{0.15}]$ calculated from the refined occupations of the Ca and P atomic sites showed good agreement with the formula calculated from chemical analysis and results of IR analysis, which confirmed the AB-type carbonated hydroxyapatite formation.

CONCLUSIONS

The carbonated hydroxyapatite with Ca/P equals 1.66±0.02, and was prepared by the interaction of the calcium hydroxide suspension with orthophosphoric acid alcohol solution in the presence of TBAOH during 2 hours. TBAOH acted as a strong base and it was actively utilized for amorphous calcium hydroxide formation. The lower degree of hydroxyapatite particle agglomeration was shown by this method. The alcohol medium was very effective for the formation of very fine amorphous calcium phosphate (particle size < 20 nm), which can be transformed into crystalline HAP by annealing at 600°C in air. The AB-type carbonated hydroxyapatite formation was verified and the calculated formula of water treated and annealed (at 600°C) HAP was $Ca_{4.64}(PO_4)_{2.83}(CO_3)_{0.17}[(OH)_{0.13}(CO_3)_{0.15}]$. Prepared carbonated calcium phosphate apatite phase was considerably instable in water whereas both the CO_3^{2-} content and TBAOH adsorbed amount decreased after immersion into water. Despite the observed particle growth, XRD analysis confirmed the strong apatite lattice deformation in annealed HAP at 600°C. The pure hydroxyapatite was created after thermal treatment at 950°C.

Acknowledgements

This work was realized within the framework of the project „Advanced implants seeded with stem cells for hard tissues regeneration and reconstruction“, which is supported by the Operational Program “Research and Development” financed through the European Regional Development Fund.

REFERENCES

[1] Olszta, JM., Cheng, X., Jee, SS., Kumar, R., Kim, YY., Kaufman, MJ., Douglas, EP.,

Gower, LB.: Material Science Engineering R, vol. 58, 2007, p. 77
[2] Bernard, L., Freche, M., Lacout, JL., Biscant, B.: Powder Technology, vol. 103, 1999, p. 19
[3] Afshar, A., Ghorbani, M., Ehsani, N., Saeri, MR., Sorrell, CC.: Materials and Design, vol. 24, 2003, p. 197
[4] Smiciklas, I., Onjia, A., Raicevic, S.: Sep. Purif. Technol., vol. 44, 2005, no. 2, p. 97
[5] Pang, YX., Bao, X.: J. Europ. Ceram. Soc., vol. 23, 2003, p. 1697
[6] Landi, E., Celotti, G., Legroscino, G., Tampieri, A.: Journal of the European Ceramics Society, vol. 23, 2003, p. 2931
[7] Krajewski, A., Mazzocchi, P., Buldini, PL., Ravaglioli, A., Tinti, A., Taddei, P., Fagnano, C.: Journal of Molecular Structure, vols. 744-747, 2005, p. 221
[8] Rajabi-Zamani, AH., Behnamghader, A., Kazemzadeh, A.: Materials Science and Engineering C, vol. 28, 2008, p. 1326
[9] Tung, MS., O'Farrell, TJ.: Colloids and Surfaces A: Physicochemical and Engineering Aspects, vol. 110, 1996, p. 191
[10] Ikawa, N., Oumi, Y., Kimura, T., Ikeda, T., Sano, T.: Journal of Materials Science, vol. 43, 2008, p. 4198
[11] Crooks, JE., Donnellan, JP.: J. Org. Chem., vol. 55, 1990, p. 1372
[12] Mayer, V.: Rozbor surového železa a oceli. Praha : SNTL, 1956
[13] El Hammari, L., Merroun, H., Coradin, T., Cassaignon, S., Laghzizil, A., Saoiabi, A.: Materials Chemistry and Physics, vol. 104, 2007, p. 448
[14] Coates, J.: Interpretation of Infrared Spectra. A Practical Approach. Chichester : John Wiley & Sons Ltd, 2000
[15] www.sigmaaldrich.com/irspectrumTBAOH 40%H2O
[16] Panda, RN., Hsieh, MF., Chung, RJ., Chin, TS.: Journal of Physics and Chemistry of Solids, vol. 64, 2003, p. 193
[17] Dorozhkin, SV.: Acta Biomaterialia, vol. 6, 2010, p. 4457
[18] Slosarczyk, A., Paszkiewicz, Z., Paluszkiewizc, C.: Journal of Molecular Structure, vols. 744-747, 2005, p. 657
[19] Nyquist, RA., Kagel, RO.: Infrared spectra of inorganic compounds. New York and London : Academic Press, 1971
[20] Hunter, BA., Howard, CJ.: LHPM—A Computer Program for Rietveld Analysis of X-ray and Neutron Powder Diffraction Patterns. Lucas Heights, Research Laboratories, Australia, 2000
[21] Ivanova, TI., Frank-Kamenetskaya, OV., Kol'tsov, AB., Ugolkov, VL.: Journal of olid State Chemistry, vol. 160, 2001, p. 340
[22] Wilson, RM., Elliott, JC., Dowker, SEP., Smith, RI.: Biomaterials, vol. 25, 2004, p. 2205
[23] Wilson, RM., Dowker, SEP., Elliott, JC.: Biomaterials, vol. 27, 2006, p. 4682